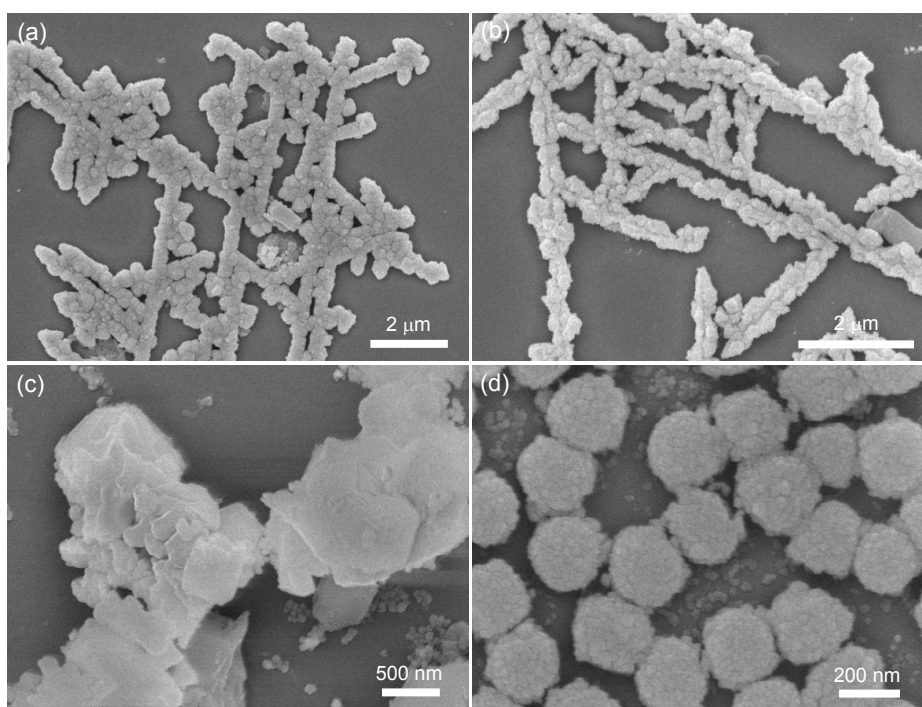


## Electronic Supplementary Information

### Hundreds of milligrams of Cr(VI) adsorbed on each gram of $\text{Cu}_2\text{O}@\text{Cu}$ fractal structures: kinetics, equilibrium, and thermodynamics

Ji Ma, Yunguo Wang, Wei Liu, Yunhao He, Qinglei Sun, Sizhi Zuo-Jiang, and  
Kezheng Chen\*

Lab of Functional and Biomedical Nanomaterials, College of  
Materials Science and Engineering, Qingdao University of  
Science and Technology, Qingdao 266042, China.



**Fig. S1** SEM images of  $\text{Cu}_2\text{O}@\text{Cu}$  products prepared at (a) 140 °C for 3h, (b) 140 °C for 6h, (c) 140 °C with cupric nitrate/urea molar ratio of 1:3 for 12h, and (d) 160 °C with cupric nitrate/urea molar ratio of 1:1 for 12h.

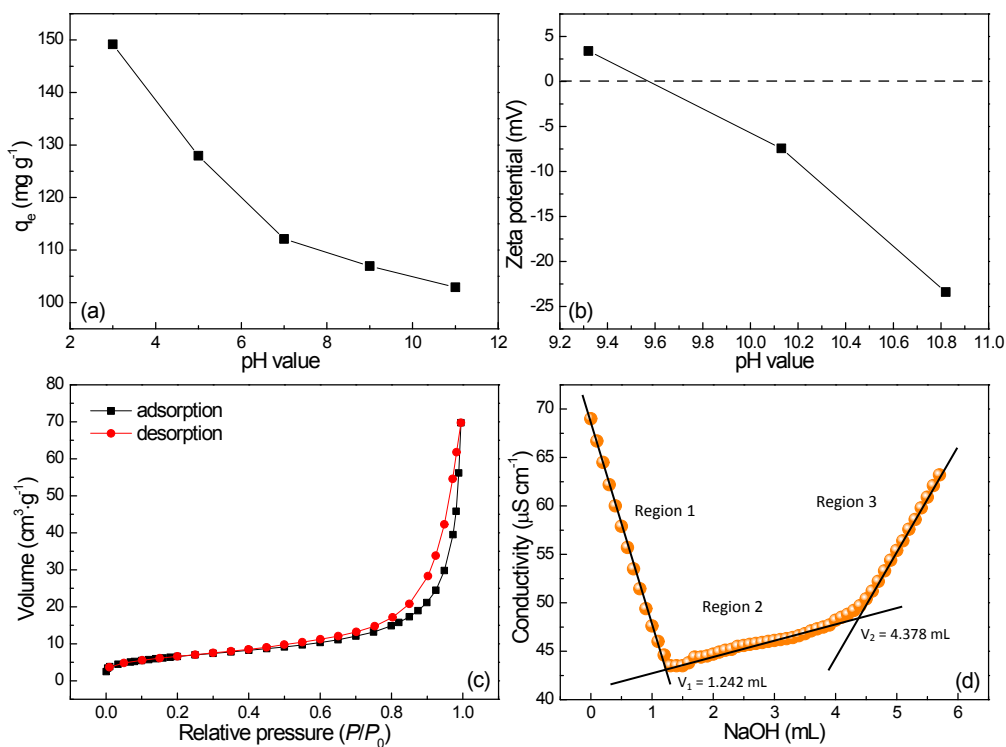


**Fig. S2** (a) Effect of pH values on the equilibrium adsorption capacity for the  $\text{Cu}_2\text{O}@\text{Cu}$  product with initial  $\text{Cr(VI)}$  concentration of  $100 \text{ mg L}^{-1}$ . (b) pH-dependent zeta potential values of the  $\text{Cu}_2\text{O}@\text{Cu}$  product in aqueous solution. (c) Nitrogen adsorption-desorption isotherm, and (d) conductometric titration of the  $\text{Cu}_2\text{O}@\text{Cu}$  product.

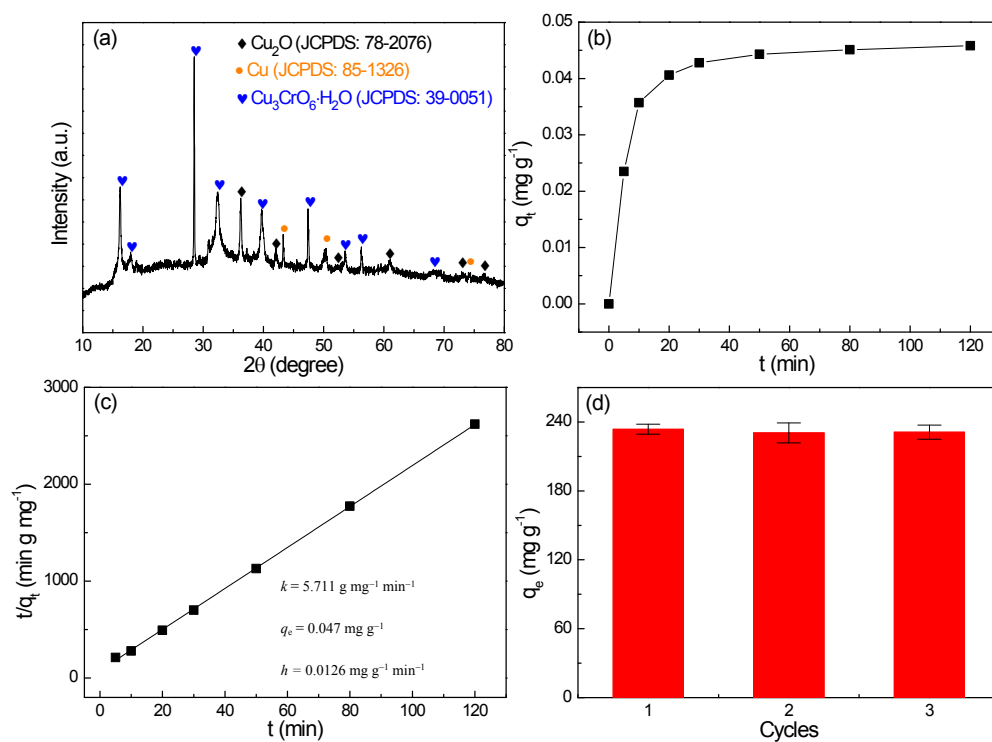


**Fig. S3** (a) XRD pattern of the  $\text{Cu}_2\text{O}@\text{Cu}$  product after  $\text{Cr}(\text{VI})$  adsorption. (b) The kinetics of  $\text{Cr}(\text{VI})$  adsorption onto the product with an initial concentration of  $50 \mu\text{g L}^{-1}$  at 293 K. (c) A linear plot of the pseudo-second-order model. (d) Equilibrium adsorption capacity of  $\text{Cr}(\text{VI})$  on the product at 293 K during 3-cycled desorption and reusability.